Evaluation of the annealing effect of proton-exchanged LiTa03 optical waveguides by the line-focus-beam ultrasonic material characterization system

doi: 10.1063/1.1496122

Evaluation of the annealing effect of proton-exchanged $LiTaO_3$ optical waveguides by the line-focus-beam ultrasonic material characterization system

Masahito Miyashita and Jun-ichi Kushibiki[a)]
Department of Electrical Engineering, Tohoku University, Sendai 980-8579, Japan

(Received 1 April 2002; accepted for publication 30 May 2002)

We established an experimental procedure and collected basic data to evaluate the annealing process and effects for proton-exchanged $LiTaO_3$ optical waveguides using the line-focus-beam ultrasonic material characterization (LFB-UMC) system in a frequency range of 100 to 300 MHz. Twelve Z-cut $LiTaO_3$ substrates were proton-exchanged at 260 °C for 14 min in a pyrophosphoric acid solution and annealed at 420 °C for various periods from 10 sec to 24 h. The leaky surface acoustic wave (LSAW) velocities were decreased by the proton exchange, and were then increased and recovered by annealing in all propagation directions as the annealing time increased. The Y-axis propagation is most useful for an evaluation. The LSAW velocities decrease with an increase of the product fH, obtained from the frequency dependences and proton-diffused layer depths analyzed by secondary-ion mass spectrometry. Gradients of the fH dependences of the LSAW velocities become gentler with increases in the annealing time, corresponding to the concentrations and distributions of hydrogen and lithium ions in the proton-diffused layers. The relationships among the LSAW velocities, proton-diffused layer depths, relative concentrations of hydrogen ions at the specimen surfaces, and the annealing times were experimentally obtained. The measurement resolutions of the LFB-UMC system at 225 MHz to the proton-diffused layer depth, the relative concentration of hydrogen ions, and the typical annealing time for 1 min were estimated to be 4 nm, 0.2%, and 0.6 sec. © *2002 American Institute of Physics.* [DOI: 10.1063/1.1496122]

I. INTRODUCTION

The line-focus-beam ultrasonic material characterization (LFB-UMC) system can quantitatively evaluate and analyze the elastic properties of specimens by measuring the propagation characteristics (phase velocity and propagation attenuation) of leaky surface acoustic waves (LSAWs) excited on the water-loaded specimen surface.[1–11] We have proposed the system as a characterization and evaluation technology for fabrication processes and systems of waveguide-type optoelectronic devices.[3–5] We used the fabrication process of proton exchange in a pyrophosphoric acid solution for optical waveguides[12–15] and experimentally related the LSAW velocities measured for as-proton-exchanged Z-cut $LiTaO_3$ optical waveguides to the depths of the proton-exchanged layers and the process parameters of the proton exchange (temperature, time, and diffusion coefficient).[5] We successfully demonstrated that this ultrasonic method yields extremely high-measurement resolution for the proton-exchanged layer depths and the process parameters.[3,5] It is necessary to anneal as-proton-exchanged $LiTaO_3$ substrates in the fabrication processes of $LiTaO_3$ optical waveguides with low-propagation loss by the proton exchange method.[13]

In this article, we apply the LFB-UMC system to the evaluation of Z-cut $LiTaO_3$ proton-diffused layers fabricated by proton exchange and annealing and collect basic data to evaluate the annealing conditions and effects. The specimens were proton-exchanged at 260 °C for 14 min and then 12 Z-cut $LiTaO_3$ specimens with proton-diffused layers were prepared by changing the annealing time as a process parameter under a constant annealing temperature of 420 °C, in consideration of the usual fabrication conditions for second-harmonic generation (SHG) devices.[13–15] LSAW velocity measurements by the LFB-UMC system for these specimens were compared with analyses of the depth profiles of hydrogen and lithium and the depth measurements of proton-diffused layers by secondary-ion mass spectrometry (SIMS).

II. LFB-UMC SYSTEM

The measurement principle of the LFB-UMC system is described in the literature.[1,2] Figure 1 shows a typical transducer output $V(z)$ obtained by changing the relative distance z between the ultrasonic device and the surface of a Z-cut Y-propagating (ZY) $LiTaO_3$ substrate. Oscillation interval Δz is obtained from the $V(z)$ curve shown in Fig. 1, according to the analytical procedure of the $V(z)$ curve.[1] The LSAW velocity is accurately obtained by substituting Δz into the following equation:

$$V_{\mathrm{LSAW}} = \frac{V_W}{\sqrt{1-\left(1-\frac{V_W}{2f\cdot\Delta z}\right)^2}}, \tag{1}$$

where V_W is the longitudinal velocity in water and f is the ultrasonic frequency. The waves reflected from the bottom surface of the specimen in the measurement for thin speci-

[a)]Author to whom correspondence should be addressed.

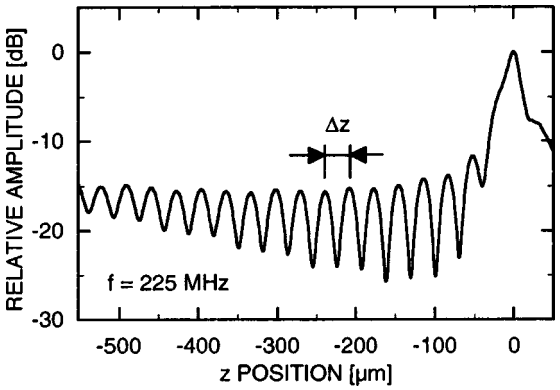

FIG. 1. Typical V(z) curve measured for a virgin Z-cut Y-propagating $LiTaO_3$ substrate at 225 MHz.

mens could affect the LSAW velocity measurements, resulting in significant measurement errors.[16,17] We used an approximated method in this article to obtain the differences in LSAW velocities measured before and after each process to avoid this problem.[3–5]

III. SAMPLE PREPARATION

Six quarter-size 0.5-mm thick substrates of 2-in. Z-cut $LiTaO_3$ wafers (optical grade, Yamaju Ceramics Co., Ltd., Seto, Japan) were used for the experiments. The fabrication conditions of optical waveguides for SHG devices were employed as the basic conditions of sample preparation, i.e., proton exchange at 260 °C for 14 min and annealing at 420 °C for 1 min.[13–15] The SHG devices were also annealed at 420 °C for 6 h in the fabrication process.[14,15] Therefore, the annealing time is taken here as a process parameter. First, six Z-cut $LiTaO_3$ substrates were proton-exchanged in a pyrophosphoric acid solution using an Al dry block bath and a 200-cm^3 SiO_2 glass beaker.[5] Each proton-exchanged substrate was then sandwiched between two 40 mm×90 mm ×2 mm graphite plates and annealed twice in air at 420 °C using an infrared ray gold image furnace (RHL-P610CP, Sinku-Riko Inc., Yokohama, Japan) for the various times shown in Table I. The annealing time is defined here as the time for which the specimen temperature was kept at 420 °C. The second annealing times were set so that the sum of the first and second annealing times for each specimen became the values shown in parentheses in Table I. The rising time from room temperature to 420 °C was set at 10 sec when the annealing time was shorter than 60 min,[14] and at 1 min for all other cases. The specimens were naturally cooled after the heating process.

TABLE I. Fabrication conditions of proton-exchanged and annealed Z-cut $LiTaO_3$ specimens. The times in the parentheses are the total annealing times after the second annealing.

Specimen number	Proton exchange	Annealing	
		First	Second
1	260 °C, 14 min	420 °C, 10 sec	420 °C, 29 min 50 sec (30 min)
2	260 °C, 14 min	420 °C, 30 sec	420 °C, 59 min 30 sec (1 h)
3	260 °C, 14 min	420 °C, 1 min	420 °C, 2 h 59 min (3 h)
4	260 °C, 14 min	420 °C, 2 min	420 °C, 5 h 58 min (6 h)
5	260 °C, 14 min	420 °C, 5 min	420 °C, 11 h 55 min (12 h)
6	260 °C, 14 min	420 °C, 10 min	420 °C, 23 h 50 min (24 h)

IV. EXPERIMENTS

A. Angular dependences

The angular dependences of the LSAW velocities were measured near the center of the $-Z$ surfaces of the specimens in 1° steps before and after each process of the proton exchange and the first and the second annealing to obtain the basic elastic properties of the fabricated specimens. The ultrasonic frequency was 225 MHz. Figure 2 shows typical measured results for the six specimens annealed for 10 sec, 1 and 10 min, and 1, 6, and 24 h. The results measured for the virgin and as-proton-exchanged specimens are also shown in Fig. 2 for comparison. In the figure, 0° and 90° correspond to the crystallographic X and Y axes. Table II shows the LSAW velocity changes relative to the results measured for the virgin specimen along the X and Y axes. The values in parentheses indicate the LSAW velocity changes relative to the LSAW velocities for the as-proton-exchanged specimens. The LSAW velocities were decreased in all propagation directions by the proton exchange. We confirmed that the LSAW velocities in the Y-axis direction for the six as-proton-exchanged specimens coincided within 2.2 m/s. This indicates that the depths of the as-proton-exchanged layers

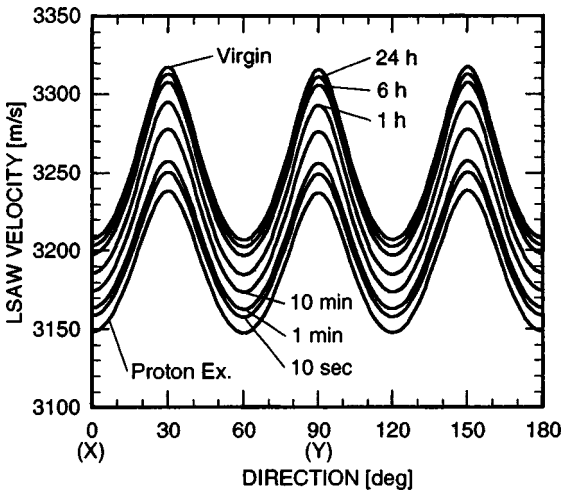

FIG. 2. Angular dependences of LSAW velocities measured for proton-exchanged and annealed Z-cut $LiTaO_3$ specimens at 225 MHz. The specimens were proton-exchanged at 260 °C for 14 min in a pyrophosphoric acid solution. The annealing process was conducted at 420 °C for 10 sec, 1 and 10 min, and 1, 6, and 24 h.

TABLE II. LSAW velocity changes at 225 MHz, relative intensities of hydrogen, proton-diffused layer depths, and gradients of fH dependences of LSAW velocities for the proton-exchanged and annealed Z-cut $LiTaO_3$ specimens.

Annealing time	LSAW velocity change [m/s]		Relative intensity of hydrogen [%]	Depth of proton-diffused layer [μm]	Gradient of fH dependence of LSAW velocity [(m/s)/(Hz m)]
	X propagating	Y propagating			
0 sec	−57.5−−59.3	−76.4−−78.6	100	0.40−0.42	−0.811
10 sec	−48.1 (+9.3)	−65.4 (+11.1)	45	0.87±0.1	−0.245
30 sec	−45.9 (+12.0)	−62.2 (+14.6)	30	1.00±0.1	−0.190
1 min	−44.2 (+15.1)	−59.4 (+19.1)	26	1.16±0.1	−0.145
2 min	−41.5 (+17.6)	−55.1 (+23.3)	25	1.37±0.1	−0.106
5 min	−35.4 (+23.3)	−43.3 (+34.4)	18	1.86±0.1	−0.056
10 min	−32.4 (+25.3)	−38.4 (+38.2)	14	2.02±0.1	−0.046
30 min	−26.1 (+31.4)	−28.2 (+48.2)	10	3.7±0.5	−0.020
1 h	−21.5 (+36.4)	−22.0 (+54.8)	6.9	5.8±0.5	−0.010
3 h	−14.6 (+44.8)	−14.4 (+64.2)	2.1	11.7±0.5	−0.002
6 h	−9.4 (+49.7)	−9.2 (+69.3)	1.2	22±0.5	0.0
12 h	−6.2 (+52.4)	−6.0 (+71.8)	0.7	38±0.5	0.0
24 h	−3.5 (+54.3)	−3.5 (+73.0)	0.3	>48	0.0

fabricated for all the specimens were almost the same.[5] The LSAW velocities increased after the annealing process and displayed a tendency to recover in all propagation directions with an increase in the annealing time, approaching the original LSAW velocities of the virgin specimens. We found that the LSAW velocity changes due to annealing were almost constant in all propagation directions in the specimens annealed for more than one hour. We suggest that velocity measurements of LSAWs propagating in the Y-axis direction are most suitable for evaluating the annealing process conditions, based on the fact that the LSAW velocity changes obtained here by annealing were generally maximum in the Y axis.

B. Frequency dependences

The propagation characteristics of LSAW velocities in layered media generally exhibit dispersion that depends upon the product fH of the ultrasonic frequency f and the layer thickness H.[1,3–5] The frequency dependences of the LSAW velocities were measured near the center of the $-Z$ surfaces of the specimens in 1 MHz steps from 100 to 300 MHz after each process to determine the dispersion characteristics of the LSAW velocities caused by formation of the proton-diffused layers. The LSAW propagation direction was selected along the Y axis. Figure 3 shows the typical measured results for specimens annealed for six annealing times, i.e., 10 sec, 1 and 10 min, and 1, 6, and 24 h. The ordinate shows the LSAW velocity changes relative to the results measured for the virgin specimen, where 0 m/s corresponds to 3318 m/s. The LSAW velocities measured for the as-proton-exchanged specimens exhibited dispersion that decreased linearly in proportion to the ultrasonic frequency, as described in the literature.[5] The LSAW velocities became higher after annealing over the frequency range used here, and the gradients of the frequency dependences of the LSAW velocities became gentler as the annealing time increased. The LSAW velocities were almost constant in the frequency range used here for an annealing process longer than 6 h. We consider that the differences in the frequency dependences of the LSAW velocities among the specimens reflect the differences in depths and concentrations of hydrogen and lithium, as described in the next section.

C. Hydrogen and lithium profiles

The hydrogen and lithium depth profiles were analyzed by SIMS to interpret the LSAW velocity changes caused by the processes. The analyzed results are shown in Fig. 4 for annealing times of 10 sec, 1 and 10 min, and 1, 6, and 24 h. The maximum analyzed depth in the SIMS examination was 48.4 μm. The abscissa in Fig. 4 shows the distance from the specimen surface into the substrate. The relative intensities of the secondary hydrogen ions in the ordinate of the figures were normalized by the intensity at the surface of the as-proton-exchanged specimen, and the relative intensities of the secondary lithium ions, by the intensity at the bulk substrate region. The results analyzed for the as-proton-exchanged specimen at 260 °C for 14 min are also shown in the figure for comparison. Hydrogen ions are distributed into the substrates by the proton exchange. The hydrogen ions

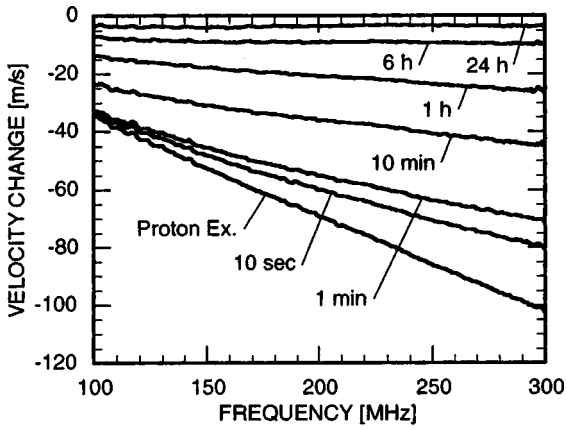

FIG. 3. Frequency dependences of LSAW velocities measured for the proton-exchanged and annealed ZY-$LiTaO_3$ specimens.

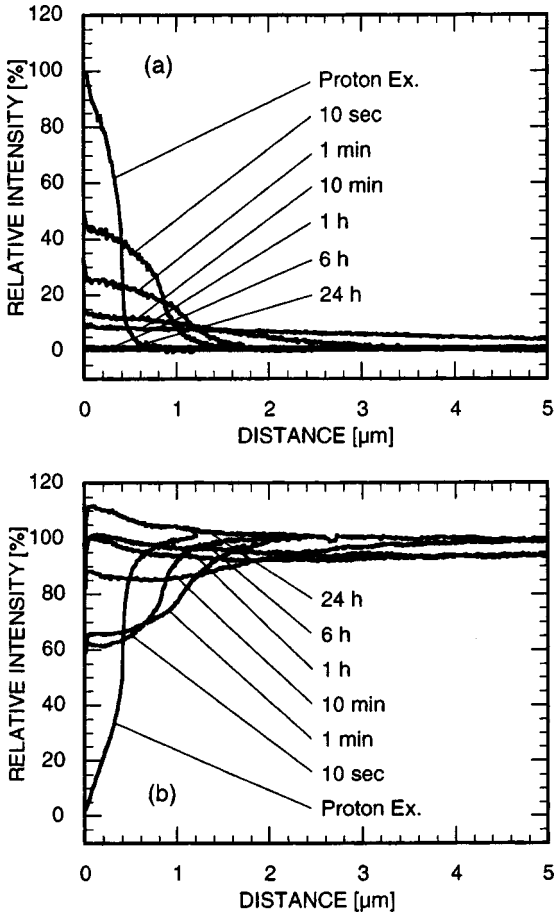

FIG. 4. Depth profiles of hydrogen and lithium ions for the proton-exchanged and annealed Z-cut $LiTaO_3$ specimens analyzed by secondary-ion mass spectrometry. (a) Hydrogen, (b) lithium.

diffuse deeper into the substrates as the annealing time increases after the initial annealing process. The hydrogen intensity for each specimen is maximum at the substrate surface. The relative hydrogen intensities at the substrate surfaces are shown in Table II. The relative surface intensities monotonically decrease as the annealing time increases. The hydrogen intensity for the specimen annealed for 24 h was almost constant at about 0.3%, which is slightly greater than that for the virgin specimen over 48 μm in depth. In contrast, the lithium intensities at the surfaces for the annealed specimens monotonically increase as the annealing time increases, but were not always minima at the surfaces. The lithium intensities at the surfaces for the specimens annealed over 30 min were clearly observed to be several percents greater than those around the bulk substrate region, with the minima at positions located beneath the surface. The depths of the proton-diffused layers were obtained by defining the position at which the hydrogen intensity becomes $1/e$ of the surface intensity in Fig. 4 and are shown in Table II. Errors in the determined depths of the proton-diffused layers were estimated to be about $\pm 0.1-0.5$ μm depending on the annealing time. The hydrogen ions introduced by the proton exchange rapidly diffuse into the substrate as the annealing time increases, and the lithium ions are transported towards the surface from the deeper region. The proton-diffused layer

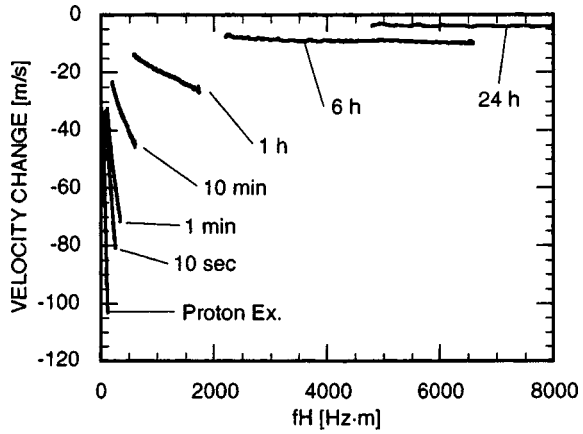

FIG. 5. fH dependences of LSAW velocities for the proton-exchanged and annealed ZY-$LiTaO_3$ specimens.

depth then becomes deeper, and the state in the proton-diffused layer seems to approach the state of the original bulk substrate.

V. DISCUSSIONS

A. *fH* dependences

fH dependences of the LSAW velocities for the proton-exchanged and annealed Z-cut $LiTaO_3$ specimens can be obtained using the frequency dependences shown in Fig. 3 and the proton-diffused layer depths in Table II. Figure 5 shows typical results for specimens with annealing times of 10 sec, 1 and 10 min, and 1, 6, and 24 h. The fH dependences of LSAW velocities for the as-proton-exchanged specimens are also given in Fig. 5 for comparison, with almost the same gradients of -0.811 (m/s)/(Hz m). These coincide with the almost constant gradient of -0.78 (m/s)/(Hz m) in the previous work,[5] conducted under broader proton-exchange conditions with several process temperatures (220–280 °C) and times (5–30 min). In contrast, the LSAW velocities for proton-exchanged and annealed specimens became higher and the gradients of the fH dependences of LSAW velocities became gentler as the annealing time increased. The gradients of the approximated lines for the fH dependences of LSAW velocities in a frequency range from 175 to 275 MHz are listed in Table II. The annealing effect was that the gradients of the fH dependences became gentler with increases in the annealing time, exhibiting remarkably different dispersion characteristics.

The results shown in Fig. 5 can be interpreted as follows. The Rayleigh-type LSAW propagation characteristics, the fundamental surface propagation mode, used for evaluation here are strongly susceptible to the elastic properties within one wavelength depth from the specimen surface. Thus, the LSAW velocities significantly decrease as f or H increases, reflecting the relatively stronger influence of the elastic properties (with lower velocities) of the proton-exchanged and annealed layers than those of the substrates. Therefore, the fH dependences of LSAW velocities for the as-proton-exchanged specimens with different depths overlapped on a single line, as described in the literature.[5] This could be in-

terpreted by taking a simple model of a single-layered structure with a steplike elastic property and proton distribution.

However, both the proton-diffused layer depths and the concentrations and distributions of hydrogen and lithium ions changed in the proton-exchanged and annealed Z-cut $LiTaO_3$ specimens examined here, as shown in Fig. 4. The changes in the concentrations and distributions suggest corresponding changes in the elastic properties, since the elastic properties of the proton-exchanged Z-cut $LiTaO_3$ substrate have slower LSAW velocities than those of the virgin substrates.[3,5] It can therefore be presumed that the gradients of the fH dependences depend directly on the concentrations and profiles of hydrogen and lithium in the proton-diffused layers. The differences in elastic properties between the proton-exchanged and annealed specimens and the virgin Z-cut $LiTaO_3$ specimens become increasingly significant when the hydrogen concentration becomes greater and the lithium concentration is reduced; the LSAW velocity decreases, and the gradient of the fH dependence becomes steeper. In contrast, the differences in elastic properties are reduced, the LSAW velocity increases, and the gradient of the fH dependence becomes gentler when the hydrogen concentration decreases and the lithium concentration increases. The LSAW velocities for the specimens annealed for more than 6 h were almost constant within the fH ranges. They showed no fH dependences because the intensities of hydrogen distributed almost uniformly over the depth of one LSAW wavelength, e.g., the maximal LSAW wavelength of about 33 μm at the lowest frequency employed in this study, 100 MHz. However, the elastic properties were slightly different from those of the virgin $LiTaO_3$ substrates.

B. Relationships between LSAW velocities and process conditions

We can use the results in the previous sections to obtain the relationships among the LSAW velocity changes, annealing process times, depths of the proton-diffused layers, and relative intensities of hydrogen at the surface that are required to evaluate the annealing process by measuring the LSAW velocities with the LFB-UMC system; for example, using the results for the Y-axis propagation at 225 MHz. The diffusion characteristics in the annealing process are dominated by the initial proton distribution formed on the substrate surface and the process temperature and time. Therefore, the relationships from Table II hold for an arbitrary annealing time at 420 °C under the proton-exchanged conditions at 260 °C for 14 min in a pyrophosphoric acid solution.

It is not necessary to strictly control the annealing time under the annealing conditions of 6 h at 420 °C used in the fabrication processes of SHG devices[14,15] since the LSAW velocities are insensitve to it. The LSAW velocities and corresponding waveguide parameters vary significantly with the annealing time in the annealing conditions of 1 min at 420 °C used for the fabrication of optical waveguides,[13–15] with a sensitivity of 5.5 sec/(m/s) around 1 min. Therefore, it is very important to evaluate the fabrication conditions and sytems, to feed the results back, and to accurately control the process conditions in order to realize optical waveguides with the desired properties.

TABLE III. Sensitivity and resolution of the proton-diffused layer depth, relative hydrogen intensity, and annealing time by LSAW velocity measurements.

	LSAW velocity	Depth	Intensity	Annealing time
Sensitivity	···	0.042 μm/(m/s)	2.0%/(m/s)	5.5 sec/(m/s)
Resolution	0.1 m/s	0.0042 μm	0.2%	0.6 sec

The resolution in LSAW velocity measurements around 3300 m/s is estimated to be within ± 0.1 m/s, since the measurement resolution of the LSAW velocity is $\pm 0.002\%$ at any chosen point.[18] The sensitivities and resolutions for the annealing times, the proton-diffused layer depths, and the relative intensities of hydrogen at the specimen surface obtained by LSAW velocity measurements are then estimated, as shown in Table III. The LFB-UMC system provides extremely high sensitivity and resolution for the evaluation of each parameter.

VI. SUMMARY

We conducted an experimental investigation in this article to collect basic data and establish an experimental procedure, which are required to evaluate the annealing process and effect of proton-exchanged Z-cut $LiTaO_3$ optical waveguides using the LFB-UMC system. We used the annealing time (10 sec to 24 h) as a process parameter at a constant annealing temperature of 420 °C for Z-cut $LiTaO_3$ substrates proton-exchanged at 260 °C for 14 min in a pyrophosphoric acid solution. The LSAW velocities were measured for these specimens in a frequency range of 100 to 300 MHz by the LFB-UMC system; the depth profiles of the hydrogen and lithium ions were analyzed by SIMS; and the proton-diffused layer depths were measured.

The measured results of the angular dependences of LSAW velocities revealed that the LSAW velocity is decreased by proton exchange and is increased and eventually recovers with an increase of annealing time in all propagation directions. We also demonstrated that the Y-axis propagation should be used to evaluate the annealing process conditions as well as the proton-exchange process conditions obtained previously,[5] since it exhibited the greatest LSAW velocity change. We confirmed that the gradients of the fH dependences of LSAW velocities become gentler with increased annealing times, corresponding to the concentrations and distributions of hydrogen and lithium ions in the proton-diffused layers of the specimens. The relationships among the LSAW velocities, annealing times, proton-diffused layer depths, relative intensities of hydrogen at the specimen surfaces, and gradients of the fH dependences of LSAW velocities were experimentally obtained.

Significant changes in the acoustic constants and in the optical refractive indices and propagation losses as well as electrooptic and nonlinear optical constants were reported for proton-exchanged and/or annealed $LiNbO_3$ and $LiTaO_3$ substrates.[3–7,12,13,19–24] We are very interested in extending and applying this ultrasonic method as a future study to de-

termine the elastic properties of the proton-diffused layers and to obtain the interrelationships between the acoustic and optical properties.

This article clearly demonstrated that the LFB-UMC system is very capable of nondestructively detecting slight changes in surface properties in a surface treatment or fabrication process, such as thin film layers and implanted/diffused layers employed in the scientific and industrial fields of electronics, which could not be easily obtained by conventional methods.

ACKNOWLEDGMENTS

The authors would like to express their sincere gratitude to K. Yamamoto and K. Mizuuchi of Matsushita Electric Industrial Co., Ltd. for their helpful advice concerning preparation of the specimens, to T. Sato of the Institute for Advanced Materials Processing, Tohoku University, for analyzing the specimens by SIMS, to I. Takanaga for constructing the heat treatment system, and T. Okuzawa for constructing the fabrication system for proton exchange. This work was supported in part by a Research Grant-in-Aid from the Ministry of Education, Science and Culture of Japan.

[1] J. Kushibiki and N. Chubachi, IEEE Trans. Sonics Ultrason. **SU-32**, 189 (1985).
[2] J. Kushibiki, Y. Ono, Y. Ohashi, and M. Arakawa, IEEE Trans. Ultrason. Ferroelectr. Freq. Control **49**, 99 (2002).
[3] J. Kushibiki, M. Miyashita, and N. Chubachi, IEEE Photonics Technol. Lett. **8**, 1516 (1996).
[4] J. Kushibiki and M. Miyashita, Jpn. J. Appl. Phys., Part 2 **36**, L959 (1997).
[5] J. Kushibiki and M. Miyashita, J. Appl. Phys. **89**, 2017 (2001).
[6] P. J. Burnett, G. A. D. Briggs, S. M. Al-Shukri, J. F. Duffy, and R. M. De La Rue, J. Appl. Phys. **60**, 2517 (1986).
[7] K. Hano, N. Chubachi, and T. Sannomiya, Electron. Lett. **28**, 2306 (1992).
[8] A. Tourlog, J. D. Achenbach, and J. Kushibiki, J. Appl. Phys. **81**, 6616 (1997).
[9] J. Kushibiki, T. Okuzawa, J. Hirohashi, and Y. Ohashi, J. Appl. Phys. **87**, 4395 (2000).
[10] J. Kushibiki, Y. Ohashi, and Y. Ono, IEEE Trans. Ultrason. Ferroelectr. Freq. Control **47**, 1068 (2000).
[11] J. Kushibiki, Y. Ohashi, Y. Ono, and T. Sasamata, IEEE Trans. Ultrason. Ferroelectr. Freq. Control **49**, 905 (2002).
[12] J. L. Jackel, C. E. Rice, and J. J. Veselka, Appl. Phys. Lett. **41**, 607 (1982).
[13] K. Yamamoto, K. Mizuuchi, and T. Taniuchi, Jpn. J. Appl. Phys., Part 1 **31**, 1059 (1992).
[14] K. Mizuuchi, K. Yamamoto, and H. Sato, J. Appl. Phys. **75**, 1311 (1994).
[15] K. Mizuuchi and K. Yamamoto, J. Appl. Phys. **72**, 5061 (1992).
[16] Y. Ohashi and J. Kushibiki, Jpn. J. Appl. Phys., Part 2 **38**, L1197 (1999).
[17] J. Kushibiki, Y. Ohashi, and M. Arakawa, IEEE Trans. Ultrason. Ferroelectr. Freq. Control **47**, 274 (2000).
[18] J. Kushibiki, Y. Ohashi, and M. Arakawa, IEEE Trans. Ultrason. Ferroelectr. Freq. Control **45**, 421 (1998).
[19] E. M. Biebl, P. H. Russer, and K. Anemogiannis, *Proceedings of the IEEE Ultrasonics Symposium* (IEEE, Montreal, 1989), pp. 281–284.
[20] M. Hirabayashi, T. Yamasaki, and Y. Komatsu, Jpn. J. Appl. Phys., Part 1 **32**, 2355 (1993).
[21] S. Kakio, J. Matsuoka, and Y. Nakagawa, Jpn. J. Appl. Phys., Part 1 **32**, 2359 (1993).
[22] J. M. Zavada, H. C. Casey, Jr., R. J. States, S. W. Novak, and A. Loni, J. Appl. Phys. **77**, 2697 (1995).
[23] T. Yuhara, K. Tada, and Y. S. Li, J. Appl. Phys. **71**, 3966 (1992).
[24] X. Cao, R. Srivastava, R. V. Ramaswamy, and J. Natour, IEEE Photonics Technol. Lett. **3**, 25 (1991).